6.6 OBSERVATIONS OF THE CLOUD MICROPHYSICS & DYNAMICS IN MID-LATITUDE CIRRUS OVER SOUTH AUSTRALIA

T. Choularton, M.Gallagher*, M. Flynn, D. Figueras-Nieto, K. Bower,
Physics Department, University of Manchester Institute for Science and Technology

J.A. Whiteway, C. Cook
Department of Physics, University of Wales, Aberystwyth

J.M.Hacker
Flinders University, S.Australia.

1. INTRODUCTION

An airborne measurement campaign, EMERALD, was conducted above Adelaide in South Australia during September 2001. Concurrent in-situ sampling and remote sensing measurements were utilised to investigate cirrus dynamics, ice particle microphysics and radiation. The experimental methodology of EMERALD is highlighted in Figure 1. Two aircraft were used. One, the Airborne Research Australia (ARA) Grob 520T Egrett, flew up to heights of 14 km while carrying instruments for measuring cloud particles, humidity, temperature, ozone, turbulence, and far-IR radiative spectra. A second ARA aircraft, a Super King-Air, flew directly below the Egrett. This aircraft carried a polarization lidar, (Whiteway et al., 2002) to probe the structure of the clouds while the Egrett was deployed within the clouds. A total of ten scientific flights were obtained. Initial results will be presented providing a view of cirrus cloud structure by relating the lidar measurements to coincident, in-situ sampling of cloud microphysics. Cloud microphysics measurements were made using a SPEC Cloud Particle Imager and a DMT FSSP-100. Results will also be shown that illustrate the interaction between cloud turbulence, structure and microphysics.

2. SUMMARY OF RESULTS

The airborne lidar system is described in detail by Whiteway et al. (2002). The lidar measurements were displayed in real time (as in Fig 1) so that the mission scientist on board the King Air aircraft could direct both aircraft in-flight to regions of interest within the cloud.

Corresponding author address:
Dr.M.W.Gallagher, UMIST, Physics Dept.,
Manchester M60 1QD, UK. e-mail :
martin.gallagher@umist.ac.uk

Figure 1 shows an example of the airborne lidar measurements from the flight on 19 September 2001. This shows the lidar backscatter measurements from the entire flight as a function of time. The altitude and path of the Egret is indicated. The aircraft traversed back and forth through the same cloud system during the second half of the flight. From 5:30 onward, the Egret was flying through the same fall-streaks at decreasing heights. Also shown in this figure, the red line, is the total ice particle concentration determined by the CPI for particles larger than 10 m in diameter compared to concentrations of bullet rosette crystals (purple line). Peak concentrations during the flight exceeded 5900 L^{-1}, (over a one minute period), with a typical mean concentrations of 490 L^{-1}. The ice crystal habit and concentrations for the different regions indicated in figure 1 are broken down and listed in Table 1.

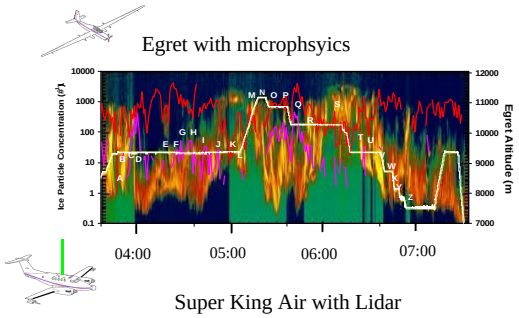

Figure 1. EMERALD Methodology. Case study from 19th September 2001. Airborne lidar measurements of backscatter parallel polarisation component from cirrus. The white line shows the height of the Egret aircraft as it was sampling ice microphysics and turbulence parameters within the cloud. The letters, (A) through (Z), correspond to various times for which samples of cloud particle images will be discussed. — is the total ice particle concentration measured by the CPI (D_p>10 mm) whilst — is the concentration of bullet rosette ice crystals (# L^{-1}).

Region	Altitude (m)	Spheroid # L^{-1}	Irregular # L^{-1}	Column # L^{-1}	Rosette # L^{-1}	Total # L^{-1}
A	8785	59.9	200.3	37.9	16.4	314.5
B	9315	0.0	0.5	0.0	0.0	0.5
C	9355	99.1	245.3	48.0	20.3	412.6
D	9348	197.8	652.4	89.9	139.1	1079.2
E	9355	74.0	318.3	33.7	8.9	428.8
F	9361	1910.1	1557.5	14.5	11.5	3488.0
G	9342	208.2	721.3	27.3	30.8	985.5
H	9345	555.5	943.2	44.7	21.7	1554.9
I	9346	141.6	501.1	139.6	18.7	799.3
J	9358	84.9	460.4	55.9	9.1	609.7
K	9372	29.5	125.1	34.8	1.5	190.8
L	9375	176.2	352.5	211.5	0.0	740.2
M	10493	66.0	88.6	16.3	1.6	172.5
O	11090	73.0	411.7	146.5	86.7	717.5
P	10877	324.5	1810.8	447.5	360.4	2940.2
Q	10295	132.2	559.4	196.6	54.5	941.2
R	10284	84.5	455.5	111.1	22.2	673.3
S	10281	14.4	104.4	16.9	6.0	141.7
T	9360	354.4	1063.1	101.2	33.7	1552.4
U	9358	296.2	875.5	147.4	14.8	1330.4
V	9276	203.2	639.5	96.6	3.7	938.6
W	8733	299.4	1041.8	143.1	4.4	1488.6
X-Z	8047	120.0	636.9	101.5	0.0	858.5

Table 1: Typical ice particle concentrations (# L^{-1}) as a function of habit at the different regions indicated in **Figure 1**.

3. DISCUSSION

It was found that the clouds consisted mostly of irregular ice crystals with spheroids, columns and bullet rosettes also present but in much lower concentrations. A few regions containing supercooled water were observed, mostly at warmer temperatures and close to the base of generating cells. Generally, however, the clouds were completely glaciated.

Figure 2 shows examples of in-situ particle images obtained in the various regions indicated in **Figure 1**. Although the majority if ice crystals encountered were small irregular particles there were distinct changes in particle characteristics between different positions within the clouds due to the large dynamical variation encountered.

In region (A-D) Prior to 4:00am (UTC) the Egrett was in the middle of a cirrus layer and sampling a mixture of large bullet rosette crystals, small irregular crystals, (the temperature at 9.5 km was –42 ^{o}C); (F) at 4:30 a sudden increase in concentration of ice crystals, mostly small irregular crystals, was detected as the Egret again entered the top of a cirrus layer at 9.5 km; (I-J) at 4:50 while flying about 500 m below cloud top there was an increase in columns; (O-P) at 5:30 at a higher cloud top (11 km) there was a mixture of large rosettes and small irregular crystals;

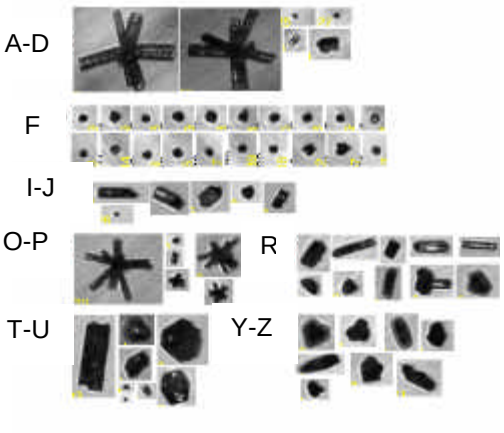

Figure 2. CPI sample images obtained by the Egret at locations indicated in **Figure 1**.

(R) in the fall-streaks below (height 10.4 km) there are some columns and mostly irregular plate crystals; (T-U) further down in the fall-streaks (height 9.5 km) there was an increase in plates and columns; (Y-Z) at the cloud base (height 7.5 km) the Egret was sampling the remains of crystals that were precipitating and evaporating at temperatures of –30 ^{0}C.

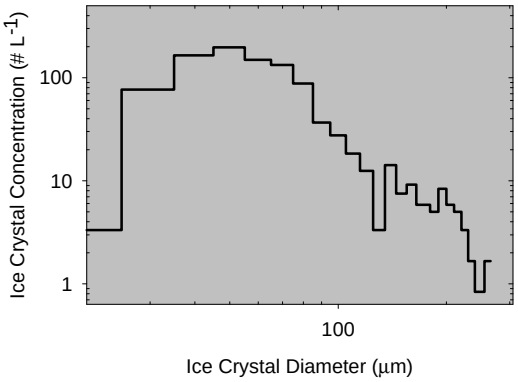

Figure 3a. Region O-P (UTC 05:26-05:37)

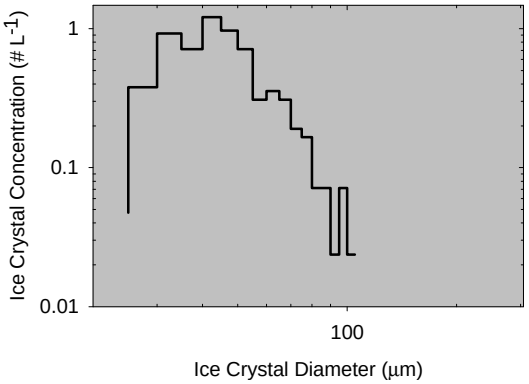

Figure 3b. Region Z (UTC 06:58-07:05)

Figure 3a shows the mean ice crystal size distribution (# L^{-1}) in regions O-P and

during the stepped descent region Z corresponding to positions at the cirrus cloud top and beneath the cirrus layer, **Figure 3b**, as indicated by the lidar in **Figure 1**. The reduction in concentration observed by the CPI for particles below 30 m is due to a roll-off in response of this instrument below this size range. Comparison with small ice crystal concentrations measured by a DMT FSSP-100 suggest a definite increase in concentrations for these smaller particles. The turbulence field as measured by the ARA 3-D high resolution turbulence BAT probe was used to determine regions of up-draft and down-draft within the cloud and associate these with the dynamical evolution and transport of ice crystals. An example of a strong downdraft episode (Region D, Figure 1) is shown in Figure 4 and Figure 5 shows the variation of columnar, spheroidal and irregular ice crystal concentrations throughout region D-E.

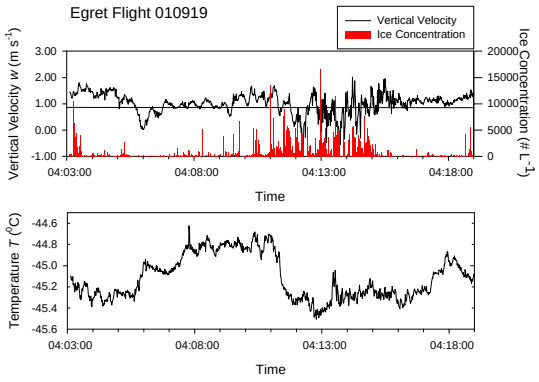

Figure 4. Region D: simultaneous turbulent vertical velocity, *w*, temperature, T, and ice crystal concentration (# L^{-1}) measured by the Egret.

These data will be used to initialise an explicit microphysics and dynamics model to investigate the evolution of cirrus structure at these latitudes.The presentation will describe details of the cloud microphysical structure as well as observation of the microphysical development including the precipitation formation processes. The factors determining the depth of penetration of the precipitation below the cloud will be investigated. The implications of the results for the computation of the radiative properties of cirrus clouds, together with their influence on water vapour distribution in the upper troposphere will be discussed.

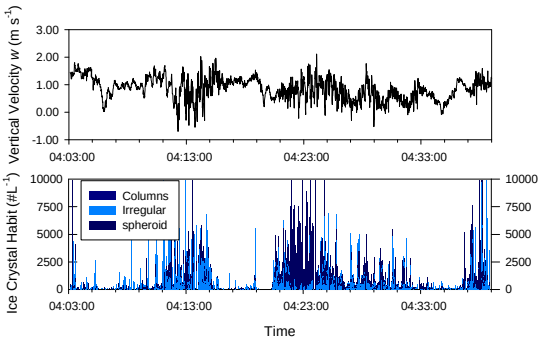

Figure 5. Region D-E: Irregular, Columnar & Spheroidal ice crystal concentration (#L^{-1}) compared to vertical velocity, *w*.

3.1 *References*

Lawson, R. P. , B. A. Baker, C. G. Schmitt, and T.L. Jensen. (2001): An overview of microphysical properties of Arctic stratus clouds observed during FIRE.ACE. *Special Issue: J. Geophys. Res.*

J.A. Whiteway ,C. Cook, T. Choularton, M.Gallagher, K. Bower, D. Figueras-Nieto & M. Flynn, (2002). Results from the EMERALD airborne cirrus measurement campaign. *International Laser Radar Conference (ILRC) , Quebec, Canada, 8-12 July, 2002.*

3.2 *Acknowledgements*

The authors gratefully acknowledge the considerable assistance by Dr.Paul Lawsson and his team at SPEC Inc., as well as the pilots & scientific staff at ARA without whom this work could not have been completed. This work was funded by the UK NERC Clouds Water Vapour & Climate Thematic Science Programme.